1

What is the quark–gluon plasma?

In this chapter, we present a pedagogical introduction to quantum chromodynamics (QCD), the quark–gluon plasma (QGP), color deconfinement and chiral symmetry restoration phase transitions in QCD, the early Universe and the Big Bang cosmology, the structure of compact stars and the QGP signatures in ultra-relativistic heavy ion collisions. Schematic figures not exploiting any mathematical formulas are utilized. Perspectives on discovering QGP on Earth (Little Bang) are also provided, with an emphasis on the common methodology used to study the early Universe (Big Bang). The issues introduced in this chapter will be elucidated thoroughly in later chapters; the appropriate references to chapters are given in boldface.

1.1 Asymptotic freedom and confinement in QCD

The hydrogen atom is composed of an electron and a proton (Fig. 1.1). Whereas the electron is a point particle within the current experimental resolution, the proton is known to be a composite particle consisting of three quarks. The quarks are fermions having not only the flavor degrees of freedom (up (u), down (d), strange (s), charm (c), bottom (b), top(t)), but also color degrees of

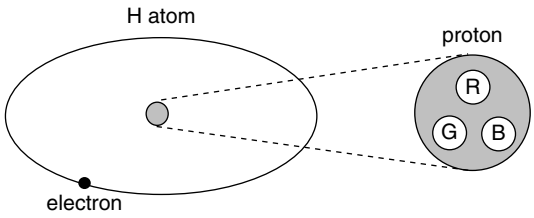

Fig. 1.1. An illustration of a hydrogen atom (H). The proton (p) is a composite object composed of three quarks with primary colors R, B and G glued together by the color gauge field (the gluon). Characteristic sizes of H and p are $\sim 10^{-10}$ m and $\sim 10^{-15}$ m, respectively.

Table 1.1. *Comparison between QED and QCD.*

	QED	QCD
Matter fermions	charged leptons,	quarks
	e.g. e^-, e^+	q^β, $\bar{q}^\beta$ $(\beta = \mathrm{R, B, G})$
Gauge bosons	photon (γ)	gluons (g)
	A_μ	A^a_μ $(a = 1,2,\ldots,8)$
Gauge group	U(1)	SU(3)
Charge	electric charge (e)	color charge (g)
Coupling strength	$\alpha = \frac{e^2}{4\pi\hbar c} = O(10^{-2})$	$\alpha_s = \frac{g^2}{4\pi\hbar c} = O(1)$

freedom (red (R), blue (B) and green (G)). Isolated color has never been observed experimentally, which indicates that quarks are always bound together to form color-white composite objects (the hadrons). Baryons (proton, neutron, Λ, $\Sigma, \ldots$, given in **Appendix H**) comprise three valence quarks, and mesons (π, ρ, K, $J/\psi, \ldots$, Table H.2) comprise a quark–anti-quark pair. They are the simplest possible constructions of hadrons, but possible multi-quark systems may exist.

The concept of color, as well as the quantum dynamics of color, was first proposed by Nambu (1966), and the theory is now called quantum chromodynamics (QCD); see **Chapter 2**. This is a generalization of quantum electrodynamics (QED) (Brown, 1995), which is a quantum theory of charged particles and the electromagnetic field. QCD (respectively QED) has gluons (the photon) as spin 1 gauge bosons that mediate the force between quarks (charged particles), as shown in Table 1.1. Although QCD and QED look similar, there is a crucial difference: whereas the photon is electrically neutral and therefore transfers no charge, the gluons are not neutral in color. The fact that gluons themselves carry color is related to the fundamental concept of non-Abelian or Yang–Mills gauge theory (Yang and Mills, 1954). The term "non-Abelian" means "non-commutative" as in $AB \neq BA$, and is realized in the color SU(3) algebra in QCD but not in the U(1) algebra in QED.

QCD provides us with two important characteristics of quark–gluon dynamics. At high energies, the interaction becomes small, and quarks and gluons interact weakly (the asymptotic freedom; see Gross and Wilczek (1973), Politzer (1973) and 't Hooft (1985)), while at low energy the interaction becomes strong and leads to the confinement of color (Wilson, 1974); see **Chapter 2**. The asymptotic freedom, which is a unique aspect of non-Abelian gauge theory, is related to the anti-screening of color charge. Because the gauge fields themselves have color,

a bare color charge centered at the origin is diluted away in space by the gluons. Therefore, as one tries to find the bare charge by going through the cloud of gluons, one finds a smaller and smaller portion of the charge. This is in sharp contrast to the case of QED, where the screening of a bare charge takes place due to a cloud of, for example, electron–positron pairs surrounding the charge. Shown in Fig. 1.2 is an illustration of the effective (or running) coupling constant in QCD (QED) with the anti-screening (screening) feature. As the typical length scale decreases, or the energy scale increases, the coupling strength decreases in QCD. This is why we can expect QGP at high temperatures, for which the typical thermal energies of the quarks and gluons are large and thus the interactions become weak; see **Chapters 3** and **4**.

Figure 1.2 also indicates that the interaction in QCD becomes stronger at long distances or at low energies. This is a signature of the confinement of color. Indeed, the phenomenological potential between a quark and an anti-quark at large separation increases linearly, as illustrated in Fig. 1.3(a). Consequently, even if we try to separate the quark and the anti-quark, they cannot be forced apart. In reality, beyond some critical distance the potential energy becomes large enough such that a new quark–anti-quark pair pops up from the vacuum. Then, the original quark–anti-quark pair becomes two pairs. In this way, quarks are always confined inside hadrons and can never be isolated in QCD. This feature is shown schematically in Figs. 1.3(b) and (c).

Because the QCD coupling strength, α_s, becomes large at long distances, we encounter a technical difficulty, i.e. we cannot adopt a perturbative method. Wilson's lattice gauge theory (Wilson, 1974) may be used to circumvent this problem. It treats four-dimensional space-time not as a continuum, but as a lattice, just as in crystals, in which quarks occupy lattice points while the gauge field occupies lattice links (Fig. 1.4); see **Chapter 5**. By this lattice discretization, one

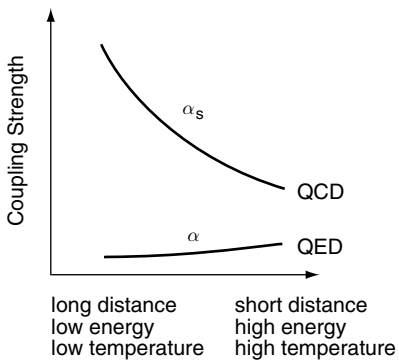

Fig. 1.2. The response of the QCD (QED) coupling strength α_s (α) with variation of the distance scale, the energy scale and the temperature.

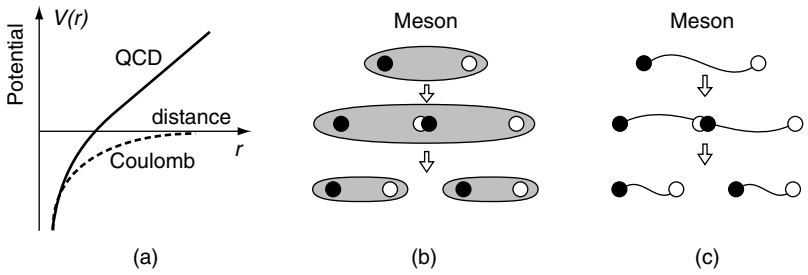

Fig. 1.3. (a) Potential between a quark and an anti-quark as a function of their separation in QCD (solid line) compared with the Coulomb potential (dashed line). (b) The quark confinement mechanism in QCD. The shaded regions represent clouds of the gluon field. The gluon configuration may be approximated as a string with a constant string tension, as shown in (c). For large enough separation, string breaking takes place.

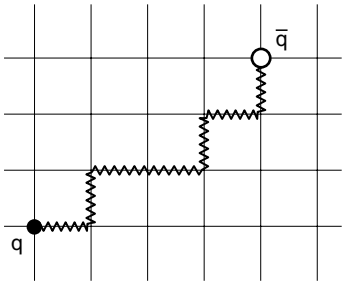

Fig. 1.4. Quarks and gluons on the space-time lattice. Quarks are defined on the lattice sites, and the gluons are defined on the lattice links.

may solve QCD utilizing Monte Carlo numerical simulations. Results confirm that the potential energy is indeed proportional to the length of the string. This agrees with that of the string model, making the idea of confinement feasible.

1.2 Chiral symmetry breaking in QCD

Another important aspect of QCD due to the large coupling at low energies is the dynamical breaking of chiral[1] symmetry; see **Chapter 6**. As first recognized by Nambu (Nambu, 1960; Nambu and Jona-Lasinio, 1961a, b), in analogy with a metallic superconductor (Bardeen, Cooper and Schrieffer, 1957), the strongly interacting QCD vacuum is a "relativistic superconductor" with the condensation of quark–anti-quark pairs. The magnitude of the condensation is measured by

[1] Chiral, originating from "chiro" (= hand in Greek), is a term which refers to the distinction between right-handedness and left-handedness.

the vacuum expectation value, $\langle \bar{q}q \rangle$, which serves as an order parameter. The masses of light hadrons are intimately related to the non-vanishing value of this order parameter.[2] Thus, one may naturally expect, in analogy with metallic superconductors, that there is a phase transition at finite T to the "normal" phase, and that the condensation and the particle spectra will experience a drastic change associated with the phase transition (**Chapter 7**).

1.3 Recipes for quark–gluon plasma

The asymptotic freedom illustrated in Fig. 1.2 immediately suggests two methods for the creation of the quark–gluon plasma (QGP).

(i) Recipe for QGP at high T (Fig. 1.5(a)). We assume that the QCD vacuum is heated in a box. At low temperature, hadrons, such as pions, kaons, etc., are thermally excited from the vacuum. Note that only the color-white particles can be excited by the confinement at low energies. Because the hadrons are all roughly the same size (about 1 fm), they start to overlap with each other at a certain critical temperature, T_c. Above this temperature, the hadronic system dissolves into a system of quarks and gluons (QGP). Note that in the QGP thus produced the number of quarks, n_q, is equal to that of anti-quarks, $n_{\bar{q}}$. The various model calculations and the Monte Carlo lattice QCD simulations yield $T_c = 150 \sim 200$ MeV (**Chapters 3** and **5**). Although this is extremely high in comparison with (for example) the temperature at the center of the Sun, 1.5×10^7 K $= 1.3$ keV, it is

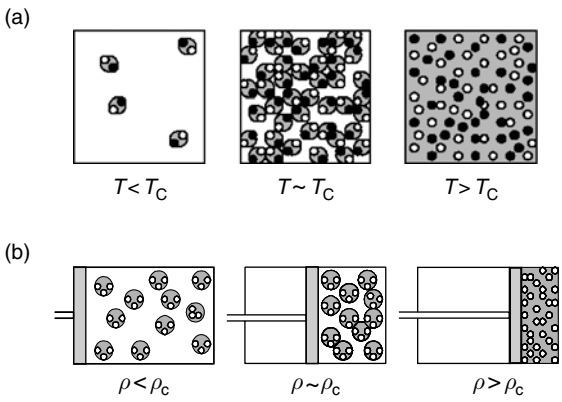

Fig. 1.5. Formation of QGP (a) at high temperature (T) and (b) at high baryon density (ρ).

[2] The concept of the order parameter was first introduced by Landau in 1937 to establish the general theory of phase transitions (see Chap. 14 in Landau and Lifshitz, 1980). Later it was applied to describe various phenomena, such as superconductivity and superfluidity.

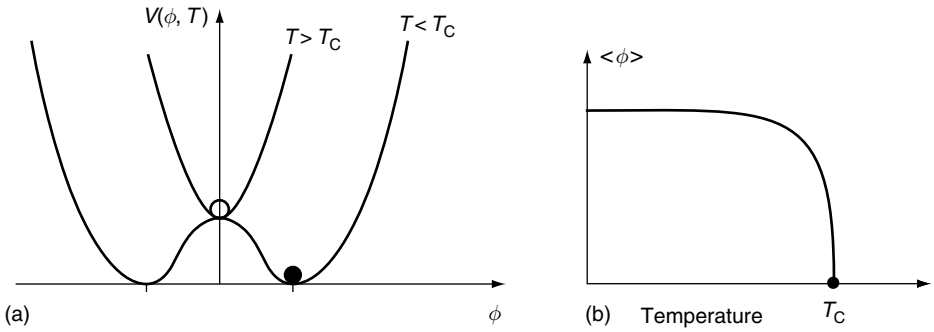

Fig. 1.6. (a) The Ginzburg–Landau potential, $V(\phi, T)$, showing the second order phase transition at $T = T_c$. (b) Behavior of the order parameter, $< \phi >$, as a function of T.

a typical energy scale of hadronic interactions and can be attained in laboratories (**Chapter 10**).

The finite T QCD phase transition may also be described by the order parameter and the corresponding Ginzburg–Landau (GL) potential (or the Landau function) if dynamical symmetry breaking and its restoration are involved. We will see such examples for center symmetry of the color SU(3) gauge group (**Chapter 5**) and global chiral symmetry of quarks (**Chapter 6**). Figure 1.6 is an illustration of the GL potential, V, as a function of an order parameter, ϕ; it also shows the behavior of the minimum of V as a function of T for the second order phase transition.

(ii) Recipe for QGP at high ρ (Fig. 1.5(b)). Let us put a large number of baryons into a cylinder with a piston and compress the system adiabatically, keeping $T \sim 0$. The baryons start to overlap at a certain critical baryon density, ρ_c, and dissolve into a system of degenerate quark matter. The quark matter thus produced is of high baryon density with $n_q \gg n_{\bar{q}}$. Model calculations show that $\rho_c = (\text{several}) \times \rho_{nm}$, where $\rho_{nm} = 0.16\,\text{fm}^{-3}$ is the baryon number density of normal nuclear matter (**Chapter 9**).

1.4 Where can we find QGP?

Based on the two recipes for high T and high ρ, we should expect to find QGPs in three places: (i) in the early Universe, (ii) at the center of compact stars and (iii) in the initial stage of colliding heavy nuclei at high energies. The last possibility, which is currently being experimentally pursued (**Chapters 15** and **16**), was already espoused during the mid 1970s (Lee, 1975).

(i) In the early Universe, about 10^{-5} s after the cosmic Big Bang (**Chapter 8**). According to Friedmann's solution (Friedmann, 1922) of Einstein's gravitational equation (**Appendix D**), the Universe experienced an expansion from a singularity at time zero. This scenario has been confirmed by the formulation of Hubble's

law for the red shift of distant galaxies (Hubble, 1929). If we extrapolate our expanding Universe backward in time toward the Big Bang, the matter and radiation become hotter and hotter, resulting in the "primordial fireball," as named by Gamow. The discovery of $T \simeq 2.73\,\mathrm{K} \sim 3 \times 10^{-4}\,\mathrm{eV}$ cosmic microwave background (CMB) radiation by Penzias and Wilson (1965) confirmed the remnant light of this hot era of the Universe. In addition, the hot Big Bang theory explains the abundance of light elements (d, He, Li) in the Universe as a result of the primordial nucleosynthesis. This idea was initiated in a paper entitled "The origin of chemical elements" by Alpher, Bethe and Gamow (1948),[3] which reminds us of the book *On the Origin of Species* by Charles Darwin published in 1859. If we go back further in time to $10^{-5} \sim 10^{-4}\,\mathrm{s}$ after its inception, the Universe is likely to have experienced the QCD phase transition at $T = 150 \sim 200\,\mathrm{MeV}$ and an electro-weak phase transition at $T \sim 200\,\mathrm{GeV}$, as shown in Fig. 1.7.

In addition, the discovery of tiny fluctuations of the cosmic temperature by COBE (COsmic Background Explorer) and by WMAP (Wilkinson Microwave Anisotropy Probe; see Bennett *et al*. (2003)) suggests the existence of a preceding inflationary period during which the Universe underwent an exponential expansion (Kazanas, 1980; Guth, 1981, Sato; 1981a, b; Peebles, 1993).

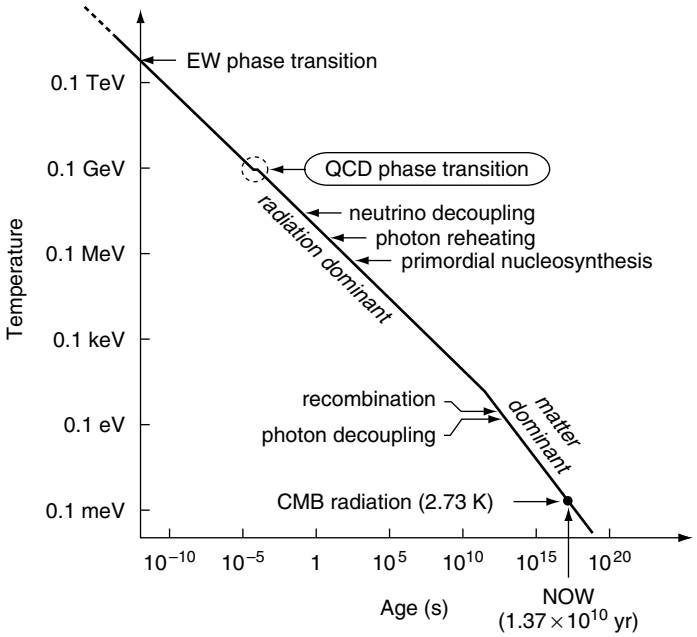

Fig. 1.7. Evolution of the Universe; the temperature of the Universe as a function of time from the moment of creation. ($0.1\,\mathrm{GeV} \simeq 1.1605 \times 10^{12}\,\mathrm{K}$.)

[3] The theory is known as the "alpha-beta-gamma theory" because the initials of the authors' names allude to ABG = ABΓ.

(ii) At the core of superdense stars such as neutron stars and quark stars (**Chapter 9**). There are three possible stable branches of compact stars: white dwarfs, neutron stars and quark stars. The white dwarfs are made entirely of electrons and nuclei, while the major component of neutron stars is liquid neutrons, with some protons and electrons. The first neutron star was discovered as a radio pulsar in 1967 (Hewish *et al.*, 1968). If the central density of the neutron stars reaches 5–10 $\rho_{\rm nm}$, there is a fair possibility that the neutrons will melt into the cold quark matter, as shown in Fig. 1.5(b). There is also a possibility that the quark matter, with an almost equal number of u, d and s quarks (the strange matter), may be a stable ground state of matter; this is called the strange matter hypothesis. If this is true, quark stars made entirely of strange matter become a possibility. In order to elucidate the structure of these compact stars, we have to solve the Oppenheimer–Volkoff (OV) equation (Oppenheimer and Volkoff, 1939), obtained from the Einstein equation, together with the equation of states for the superdense matter (**Appendix D**).

(iii) In the initial stage of the "Little Bang" by means of relativistic nucleus–nucleus collisions with heavy ion accelerators (**Chapter 10**). Suppose we accelerate two heavy nuclei such as Au nuclei ($A = 197$) up to relativistic/ultra-relativistic energies and cause a head-on collision, as shown in Fig. 1.8. In such relativistic energies, the nuclei are Lorentz-contracted as "pancakes." When the center-of-mass energy per nucleon is more than about 100 GeV, the colliding nuclei tend to pass through each other, and the produced matter between the receding nuclei is high in energy density and temperature but low in baryon density (Fig. 1.8(a)). The Relativistic Heavy Ion Collider (RHIC) at Brookhaven National Laboratory and the Large Hadron Collider (LHC) at CERN provide us with this situation (**Chapter 16**). On the other hand, when the energy is at a few to a few tens of giga-electronvolts (GeV) per nucleon, the colliding nuclei tend to stay with each other (Fig. 1.8(b)). In this case, not only high temperature but also high baryon density could be achieved.

A schematic phase diagram of QCD matter is shown in Fig. 1.9 in the plane of temperature, T, and baryon density, ρ. Possible phases of QCD and the precise

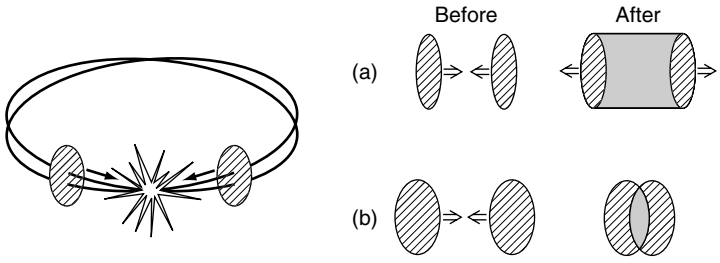

Fig. 1.8. (a) Formation of QGP at high temperature by means of relativistic nucleus–nucleus collisions with a collider-type accelerator. (b) Formation of QGP at high baryon density by means of less energetic collisions than in (a).

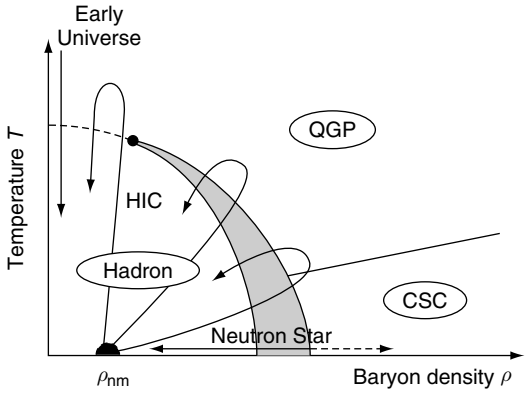

Fig. 1.9. Schematic phase diagram of QCD. "Hadron," "QGP" and "CSC" denote the hadronic phase, the quark–gluon plasma and the color superconducting phase, respectively; ρ_{nm} denotes the baryon density of the normal nuclear matter. Possible locations at which we may find the various phases of QCD include the hot plasma in the early Universe, dense plasma in the interior of neutron stars and the hot/dense matter created in heavy ion collisions (HICs).

locations of critical lines and critical points are currently being actively studied. In fact, unraveling the QCD phase structure is one of the central aims of ongoing and future theoretical and experimental research in the field of hot and/or dense QCD.

1.5 Signatures of QGP in relativistic heavy ion collisions

The relativistic heavy ion collisions are dynamic processes with typical length and time scales of order 10 fm and 10 fm/c respectively. QGP, even if it is created in the initial stage of the collision, cools rapidly, by expanding and emitting various radiation, to a hadron gas through a QCD phase transition (Fig. 1.10). Then the system eventually falls apart into many color-white hadrons (**Chapters 11, 12** and **13**). Therefore, in order to probe the QGP, we need to observe as many as possible particles/radiations emitted during the time history and then to retrace the initial formation of QGP by using the observed data. This is an analogous procedure to probing the early Universe by measuring its remnants, such as the cosmic microwave background, the abundance of atomic elements, etc.

Various QGP signatures and their relation to the real data will be discussed in detail in **Chapters 14, 15** and **16**. In order to capture the essential ideas of the signatures of QCD phase transitions, we illustrate possible candidates of signatures in Fig. 1.11 as a function of the energy density, ε, of a "fireball" initially produced in relativistic nucleus–nucleus collisions. Experimentally, the transverse energy,

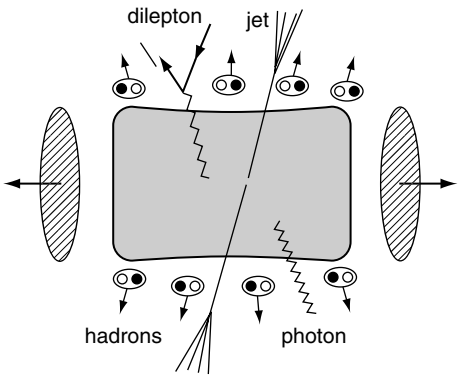

Fig. 1.10. Particles/radiations from the hot quark–hadron matter formed in a central collision between ultra-relativistic heavy nuclei.

dE_T/dy, to be measured in an electromagnetic calorimeter (**Chapter 17**) is closely connected to the energy density, ε.

In the following, (1)–(10) refer to Fig. 1.11.

(1) A second rise in the average transverse momentum of hadrons due to a jump in entropy density at the phase transition.
(2) Measurement of the size of the fireball by particle interferometry with identical hadrons (Hanbury-Brown and Twiss effect).
(3) Enhanced production of strangeness and charm from QGP.
(4) Enhanced production of anti-particles in QGP.
(5) An increase of an elliptic flow (v_2) of hadrons from early thermalization of an anisotropic initial configuration.
(6) Suppression of the event-by-event fluctuations of conserved charges.
(7) Suppression of high-p_T hadrons due to the energy loss of a parton in QGP.
(8) Modification of the properties of heavy mesons (J/ψ, ψ', Υ, Υ') due to the color Debye screening in QGP.
(9) Modifications of the mass and width of the light vector mesons due to chiral symmetry restoration.
(10) Enhancement of thermal photons and dileptons due to the emission from deconfined QCD plasma.

Obviously, the real situation is not as straightforward as that illustrated in Fig. 1.11 due to various backgrounds which tend to hide the possible signals. Also, there are theoretical indications that QGP is not a simple gas of free quarks and gluons, but rather is a strongly interacting system which may modify some of the basic ideas behind the signatures in Fig. 1.11. Nevertheless, as discussed in **Chapters 15** and **16**, the vast number of data from SPS and RHIC already provide quite promising clues which may help in pinning down the nature of QGP.